ADVANCED FUNCTIONAL MATERIALS
www.afm-journal.de

Functionalized Microparticles Producing Scaffolds in Combination with Cells

*C. A. Custódio, V. E. Santo, M. B. Oliveira, M. E. Gomes, R. L. Reis, and J. F. Mano**

The development of biologically instructive biomaterials with application for tissue regeneration has become the focus of intense research over the last years. This work reports a novel approach for the production of three-dimensional constructs for tissue engineering applications based on the assembly of chitosan microparticles exhibiting specific biological response with cells. Chitosan microparticles with a size range between 20 and 70 μm are functionalized with platelet derived growth factor (PDFG-BB). The functionalization is achieved by previous immobilization of an anti-PDGF-BB antibody, using a water-soluble carbodiimide. When incubated with a cocktail of growth factors-platelet lysates, the previously functionalized particles are able to target PDGF-BB from the protein mixture. In vitro studies are carried out focusing on the ability of these systems to promote the assembly into a stable 3D construct triggered by the presence of human adipose stem cells, which act as crosslinker agents and induce the formation of a hydrogel network. The presence of immobilized growth factors gives to this system a biological functionality towards control on cell function. It is also bioresponsive, as cells drive the assembly process of the microgel. These versatile biomimetic microgels may provide a powerful tool to be used as an injectable system for non-invasive tissue engineering applications with additional control over cellular function by creating specific microenvironments for cell growth.

1. Introduction

Sophisticated methods for the development of macroscopic three-dimensional tissue constructs have been explored in the field of tissue engineering (TE) in order to mimic the in vivo functional organization of tissues.[1–3] In contrast to the traditional "top-down" scaffolding approach, in which cells are seeded on a biodegradable polymeric scaffold, "bottom-up" tissue fabrication methods, using small units as building blocks, are potentially powerful tools to reconstruct organomimetic and uniformly dense microstructures. Microgels that can be injected into the body have recently emerged as a potential candidate for regenerative medicine by employing micro- and nanounits as building blocks to assemble into integral scaffolds.[4–6] Recent reports demonstrated the aggregation of those building blocks induced by living cells[7–10] in contrast with common in situ polymerization injectable systems that require the use of monomers and initiators typically associated with toxicity issues.

Those systems are a promising alternative for the delivery of therapeutics, including cells, as they can be injected into the body and gellify without the use of any additional crosslinking agents. Injectable microparticles (μPs) have already been used in vivo for vocal fold regeneration,[11] cartilage,[12,13] bone,[14] and adipose tissue regeneration.[15] Despite the impressive achievements reported using injectable microgels for TE applications there are still some limitations for the effective regeneration of a specific tissue and further clinical application. Technologies with a better control over microgel assembly, cell function and organization are still needed for effective applications in tissue regeneration. Control over surface functionality and interaction with the local environment are key factors for a better performance of materials used in biomedical applications.

Chitosan is a biopolymer with a wide range of biomedical applications. Of the numerous biodegradable polymers that have been studied for tissue engineering, chitosan is particularly attractive because is enzyme- degradability and biocompatibility.[16,17] An important feature that a material should display to be considered for this functional microparticles it is the availability of chemical groups for covalent modification. The chemical nature of chitosan provides many possibilities for covalent modifications which offer several possibilities for derivatization and immobilization of biologically active species.[18–20]

In this work the amino groups in the chitosan polymeric chain will be targeted for biochemical functionalization to be able to recognize specifically growth factors (GFs) from platelet derived products.

Platelet derived products include platelet lysates (PLs) and platelet rich plasma (PRP) and have been studied and used since

C. A. Custódio, Dr. V. E. Santo, M. B. Oliveira, Dr. M. E. Gomes, Prof. R. L. Reis, Prof. J. F. Mano
3B's Research Group – Biomaterials Biodegradables and Biomimetics
University of Minho
AvePark, Zona Industrial da Gandra, S. Cláudio do Barco, 4806–909, Caldas das Taipas – Guimarães, Portugal
E-mail: jmano@dep.uminho.pt
C. A. Custódio, Dr. V. E. Santo, M. B. Oliveira, Dr. M. E. Gomes, Prof. R. L. Reis, Prof. J. F. Mano
ICVS/3B's, PT Government Associated Laboratory
Braga/Guimarães, Portugal

DOI: 10.1002/adfm.201301516

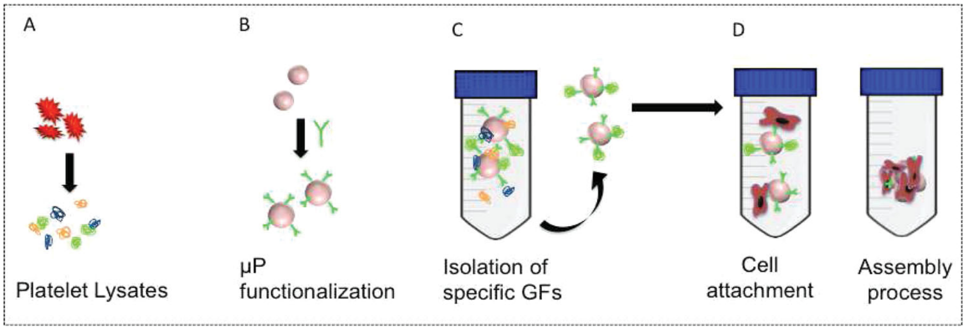

Figure 1. Schematic representation of the proposed strategy. A) GFs were released from platelet concentrates upon activation through temperature cycles. B) Chitosan microparticles were modified via antibody immobilization. C) Functionalized microparticles and GFs were mixed and non-attached GFs discarded. D) Functional particles were then mixed with cells, followed by the assembly process and the formation of a 3D construct.

the 1970s.[21] Human PLs can be generated through a simple freeze-thaw procedure of platelet units.[22] It is well established that platelets are an important source of autologous GFs that can modulate stem cell proliferation and differentiation. These GFs include platelet-derived growth factor (PDGF-BB), transforming growth factor-beta 1 (TGF-β1), insulin like growth factor (IGF-1) and basic fibroblast growth factor (bFGF).[23,24] PLs have been described as possible autologous substitutes for fetal bovine serum (FBS)-containing media for the expansion of mesenchymal stem cells (MSCs) for clinical use. Indeed, PL was reported to stimulate MSC proliferation rate and maintain their differentiation potential and immunophenotypic characteristics.[25] Before translating PL culturing to clinical use further insights into the mechanisms leading to a particular cellular response are clearly required. However major concerns were raised about the complexity of PLs and variations from batch-to-batch, making a difficult characterization process and changes in the effects of its application.[26,27] Also the use of inappropriate combinations of GFs may lead to undesirable outcomes.[28] For this reasons it is critical to develop new strategies that allow separation of the biomolecules of interest from the overall mixture present in PLs.

To optimize effectiveness in the use of PLs, controlled presentation of GFs is required using biomaterials that provide increased performance in situ.[26,28] Here we develop functional chitosan µPs able to recruit and immobilize target biomolecules as an attempt to standardize and have a better control in the use of PLs. The particles may work as an injectable system for controlled localization of GFs and cells.

Stem cells, and particularly MSCs, have generated significant interest in TE. Obtaining multipotent cells that are capable of differentiating towards different lineages from adult tissues such as bone marrow or adipose tissue is currently considered an advantageous procedure. Adipose tissue, like bone marrow (the most universal source of MSCs), is derived from the mesenchymal connective tissue and represents an abundant and accessible source of adult stem cells with the ability to differentiate along multiple lineage pathways.[29–31] In a clinical perspective it is technically straightforward to obtain cells from adipose tissue using minimally invasive procedures and with low donor site morbidity.

In the present work we hypothesize that stem cells can crosslink polymeric microparticles, if they contain specific ligands capable of binding to receptors on the cell surface (**Figure 1**). Chitosan particles were functionalized with antibodies target a particular GF of interest: PDGF-BB. PDGF, especially the BB isoform, is a well-known potent GF that stimulates the proliferation of stem cells and as a principal chemo attractant for MSCs.[32,33]

The ability of antibody functionalized µPs conjugate to specific GFs may enable major advancements in the modulation of the stem cell function. The aim of the present study is to develop injectable chitosan microgels composed by integrating small units into well-defined, multifunctional constructs in which each of these units can potentially be functionalized with different antibodies and autologous GFs, thus creating the desired cell microenvironment. This allows additional control over cell-material interactions and modulates stem cell function, facilitating tissue regeneration and integration within the host.

2. Results

2.1. Functionalization of Chitosan Microparticles

Chitosan particles have been proposed for tissue engineering and regenerative medicine due to their processability, cationic character of chitosan and their ability to be further chemically modified. The availability of primary amines on chitosan surface and carboxylic groups on proteins makes amine coupling a commonplace. In the present work, antibodies were tethered via covalent binding by formation of amide bonds between amino groups on the chitosan and carboxyl groups on the antibodies, using a water-soluble carbodiimide (EDC) (**Figure 2**a).

The frequency distribution of the diameter of the produced microparticles was analyzed (n = 49). The size distribution of the microparticles is represented in Figure 2b. The size of the microparticles ranged from 20 to 80 µm. The final average diameter of the microparticles is 41.7 ± 18.2 µm. (Figure 2b). Particles functionalized with a fluorescent antibody were imaged under fluorescence microscopy. (Figure 2c) SEM images indicated that chitosan µPs exhibit homogeneous and spheroidal shape and rough surface (Figure 2d,e).

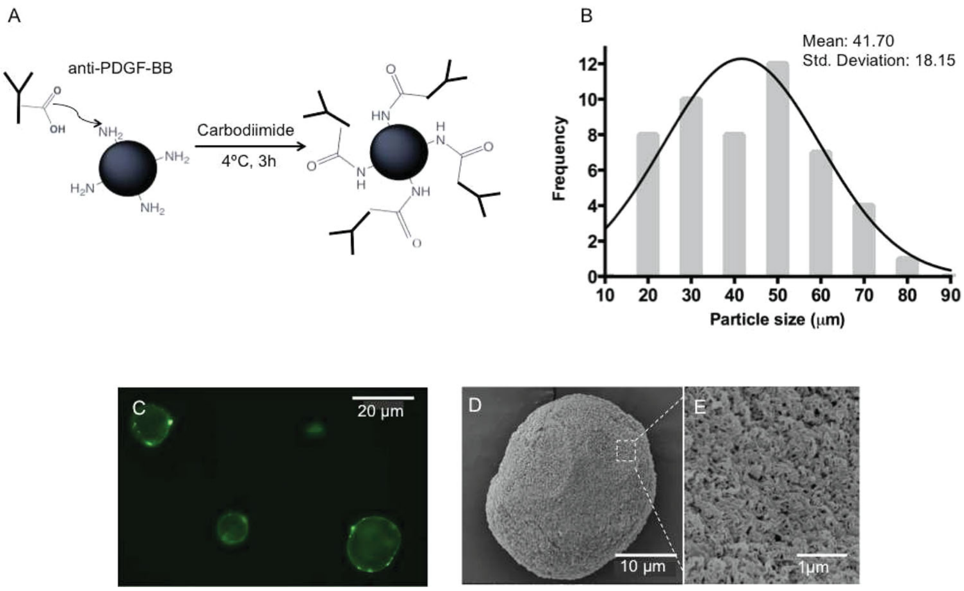

Figure 2. A) Schematic representation of antibody immobilization process on the chitosan μPs. The carboxyl group in the antibody is activated with EDC to form an active ester group that spontaneously reacts with primary amines in the chitosan particles to form an amide bond. B) Histogram of the distribution of microparticles size ($n = 49$). C) Fluorescence microscopy of chitosan μPs functionalized with Alexa fluor 488 antibody. D) SEM image of a representative chitosan μP. E) SEM image of a representative area of the particle surface.

2.1.1. Growth Factor Recruitment from Platelet Lysates

Plain chitosan generally shows limitations in supporting protein adsorption, cell adhesion and proliferation. Therefore it represents an advantageous platform for controlled protein binding and cell adhesion upon functionalization.[18–20] The present strategy involves the modification of chitosan particles with an immobilized antibody for recruitment of specific GFs in solution. Functionalized particles were resuspended in an enriched protein concentrate- PLs. Quantification of the immobilization process was performed through an ELISA assay, in order to determine the GFs content in solution after incubation with the μPs. **Figure 3** shows the concentrations of remaining PDGF-BB, TGF-β1, and VEGF in the PL dispersion.

The concentration of PDGF-BB in solution decreased significantly from a total of approximately 22.81 ± 3 ng mL^{-1} in the original protein concentrate to 7.2 ± 2 ng mL^{-1} in the PL remaining solution. Concerning TGF-β1 and VEGF, other important GFs present in high concentrations in the original PLs, a slight but not significantly decrease was observed after incubation chitosan μPs functionalized with anti-PDGF-BB. On average, TGF-β1 and VEGF decreased from 22.15 ± 2 ng mL^{-1} to 18.09 ± 2.5 ng mL^{-1} and VEGF from 29.28 ± 1.8 ng mL^{-1} to 23.69 ± 0.9 ng mL^{-1} respectively.

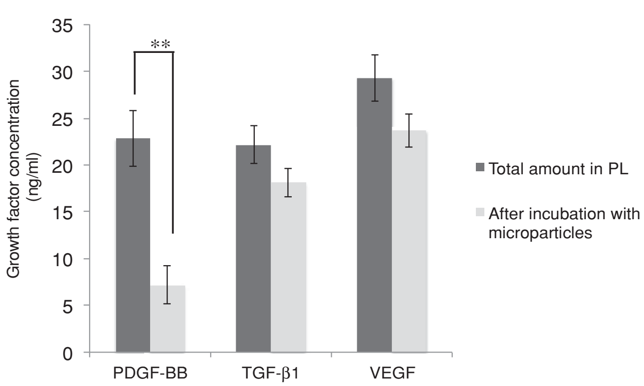

Figure 3. Quantification of concentration of three different GFs present in high concentrations in the original PLs (PDGF-BB, TGF-β1, and VEGF), before and after incubation with functionalized chitosan μPs. Results are expressed as mean ± standard deviation with $n = 3$ for each bar. * indicate statistically significant differences ($p < 0.05$).

2.2. Assembly of the 3D Construct

The use of agglomerated chitosan microparticles to produce scaffolds for tissue engineering applications has been already exploited. In the present study, an attempt was made to engineer particles able to recruit specific proteins to its surface, aiming a better control in cell function.[34] The in vitro attachment of hASCs to chitosan μPs and the assembly process were examined. The assembly process after seeding was followed for up to 24 h and the obtained results are summarized in **Table 1**. **Figure 4**a shows that, after 90 min, an aggregation of functionalized particles dictated by the presence of cells was already formed. On the other hand, controls were not able to form a stable structure and particles remain dispersed in the tubes or forming small aggregates, even after 24 h (Table 1). Fluorescence microscopy revealed that cells readily adhere to the particles, forming a layer of viable cells and delineating the shape of the chitosan μPs (Figure 4b).

2.3. Dynamic mechanical analysis (DMA)

Dynamic mechanical analysis, DMA, is an adequate tool to characterize the mechanical/viscoelastic properties of

Table 1. Macroscopic observation of the assembly process of the tested conditions at different time points up to 24 h of culture.

Formulations	90 min	12 h	24 h
μP	dispersed particles	dispersed particles	dispersed particles
μP+PL	small aggregates	3D construct	small aggregates
μP+anti-PDGF-BB	small aggregates	small aggregates	small aggregates
μP+anti-PDGF-BB+PL	aggregates	3D construct	3D construct

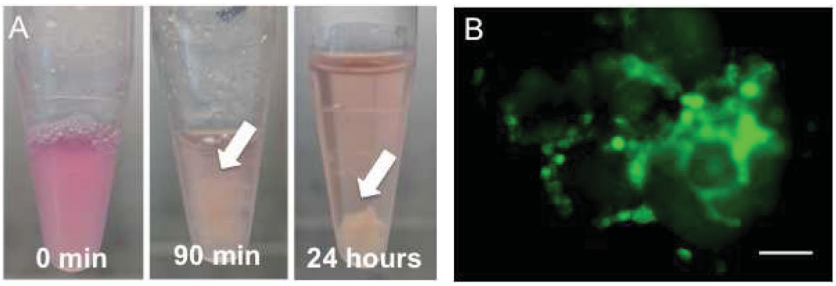

Figure 4. A) Macroscopic figures of the assembly process at different time points of the constructs containing chitosan μPs functionalized with PDGF-BB cultured in vitro up to 24 h. B) Live/dead assay after 24 h incubation. Scale bar represents 50 μm.

polymeric materials.[35,36] DMA was performed to study the effect of the culture time in the properties of the construct. Experiments were performed in a hydrated environment (PBS) and 37 °C in order to access how samples behave in a physiological-like environment. The storage modulus (E') of all samples tends to increase with increasing frequency. The mechanical behavior was assessed throughout a physiological relevant frequency range (0.1–10 Hz). The reinforcement of constructs with cells was evaluated in three different culture times: 7, 14, and 21 days (**Figure 5**a). Clearly, one can observe a systematic increase in E' for increasing culture times. Such behavior is accompanied by a decrease in the loss factor, tan δ (Figure 5b).

2.4. Cell/Microparticles Interaction

The detailed morphology of the cells in the constructs was characterized by confocal microscopy and SEM. **Figure 6** shows a representative view of the construct after 3, 7, 14, and 21 days in culture, indicating a homogeneous cell distribution within the construct. After 7 days in culture a significant number of cells was found to have migrated inside the

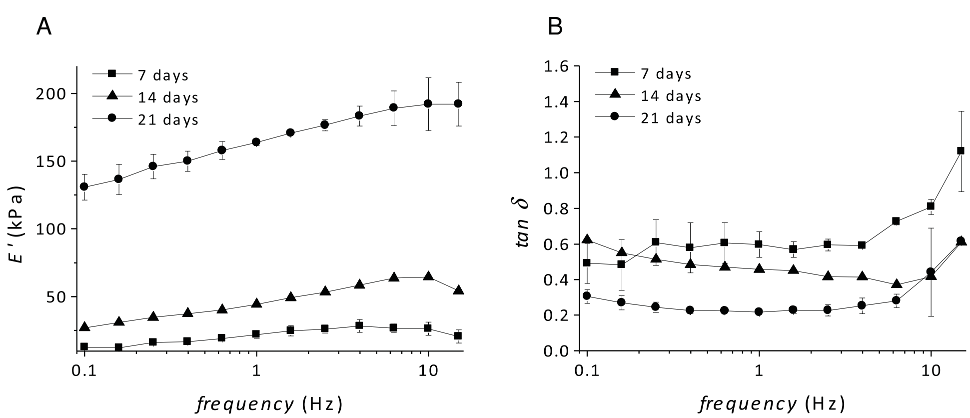

Figure 5. Representative curves of dynamic mechanical analysis of the constructs after 7, 14, and 21 days in culture, as function of the applied frequency, measured at 37 °C during immersion in PBS. A) Storage modulus (E'). B) Loss factor (tan δ).

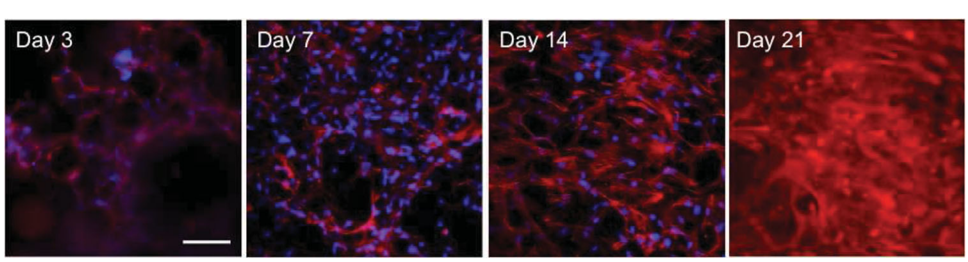

Figure 6. Fluorescence microscopy figures of representative portions of the assembled scaffolds at days 3, 7, 14, and 21, demonstrating the presence of a cellular network within the chitosan μPs. Blue color (DAPI) corresponds to cells nuclei; red color (Phalloidin) is attributed to the stained cells cytoskeleton. Scale bar represents 100 μm.

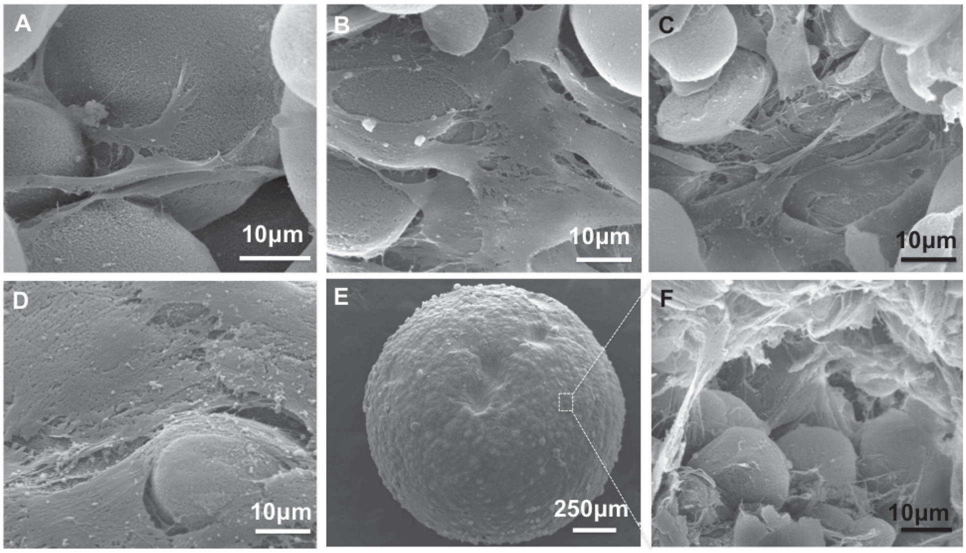

Figure 7. SEM images of representative areas of the constructs in culture after A) 24 hours; B) 3 days; C) 7 days; D) 14 days. E) General overview of the construct after 21 days in culture. F) Representative area of the inner part after 21 days in culture.

3D structure. At day 14, cells covered the majority of the particles surface and a dense cell layer was formed by day 21. These outcomes demonstrate that cells proliferated well within the construct with increasing culture time.

SEM was used to further investigate cell morphology and distribution on the assembled functionalized particles and constructs. Results showed that cells adhere well on the surface of the particles functionalized with PDGF-BB after 24 h in culture (**Figure 7**a). Several cells exhibit a spindle-like morphology on the surface of the μPs forming connecting points between particles. After 14 days in culture, cells form a confluent layers in the surface of the construct (Figure 7d), demonstrating that the construct provides an appropriate environment for cell proliferation. The microgel obtained by culturing the constructs at the bottom of a falcon tube presented a closely spherical shape (Figure 7e). Figure 7f shows the inner part of the construct after 21 days in culture at higher magnification where is possible to observe an effective colonization of the structure by the cells.

The morphological observations by the confocal microscopy and SEM clearly indicate that the cells can attach and proliferate well on the highly interconnected 3D structure. In addition, it was noted that cells are homogenously distributed within the structures. These structures are the result of PDGF-BB functionalized μPs with associated cells, between which abundant extracellular matrix could be clearly visualized.

2.5. Cell Viability and Cell Proliferation

Biological activity of the obtained constructs was assessed up to 21 days by live/dead assay, Alamar blue assay, and DNA quantification.

Regarding the cell viability assessment, results show that cells are able to remain viable in the constructs up to 21 days. Results of a live/dead assay to the constructs after 21 days in culture (**Figure 8**a,b) show a strong green fluorescent staining which indicates that the majority of the cells are alive outside and in the core of the construct.

Figure 8c shows that from day 3 to day 7, there is a statistically significant decrease on cell viability, which remained stable throughout the remaining culture period. Additionally, the DNA quantification assay confirmed that the cell number in the construct was significantly increased when the culture time was prolonged from 14 to 21 days (Figure 8d).

2.6. Histological Analysis and Immunostaining

H&E stained sections allow the visualization of the cell distribution and the deposition of extracellular matrix within the 3D constructs. Representative sections are shown in **Figure 9**a. Immunolocalization of PDGF-BB within the construct is shown in Figure 9b. The determination of PDGF-BB in the constructs was performed in order to determine the distribution of immobilized GF in the assembled materials during early culture periods, as well as the quantification of PDGF-BB secreted by the entrapped hASCs.

Histological examination of the sections indicated that the cells were evenly distributed throughout the constructs and that the cells were able to infiltrate, adhere, and proliferate into the inner parts of the construct (Figure 9a). During early culture periods, the cells clearly delineate the spheroidal shape of the particles, thus demonstrating their adhesion to the surface of the functionalized carriers. It is clear that the structure gains stability with time, which leads to increase in cell grow and higher ECM deposition, particularly at day 21 of culture. The presence of PDGF-BB in the constructs was assessed by the immunolocalization observed in Figure 9b. During early culture periods, immunostaining of PDGF-BB confirmed the presence of this GF immobilized on the surface of chitosan μPs, as demonstrated by the outlining of the spheroidal shape of the particles. This staining was also homogeneously distributed

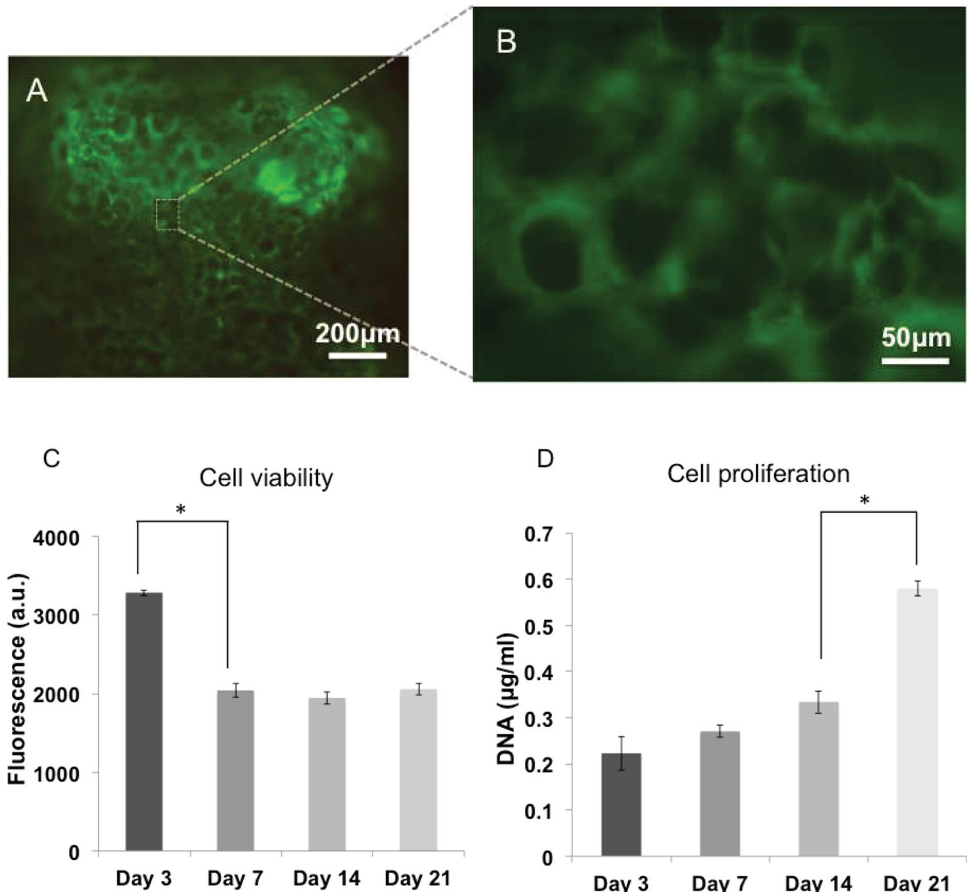

Figure 8. A,B) Fluorescent Live/Dead assay image of a construct after twenty-one days of in vitro culture. A) Overview of the construct. B) Core of the construct. C) Alamar blue viability assay and D) DNA quantification of the constructs containing chitosan µPs functionalized with PDGF-BB cultured in vitro up to 21 days with hASCs. Results are expressed as mean ± standard deviation with $n = 3$ for each bar. * indicate statistically significant differences ($p < 0.05$)

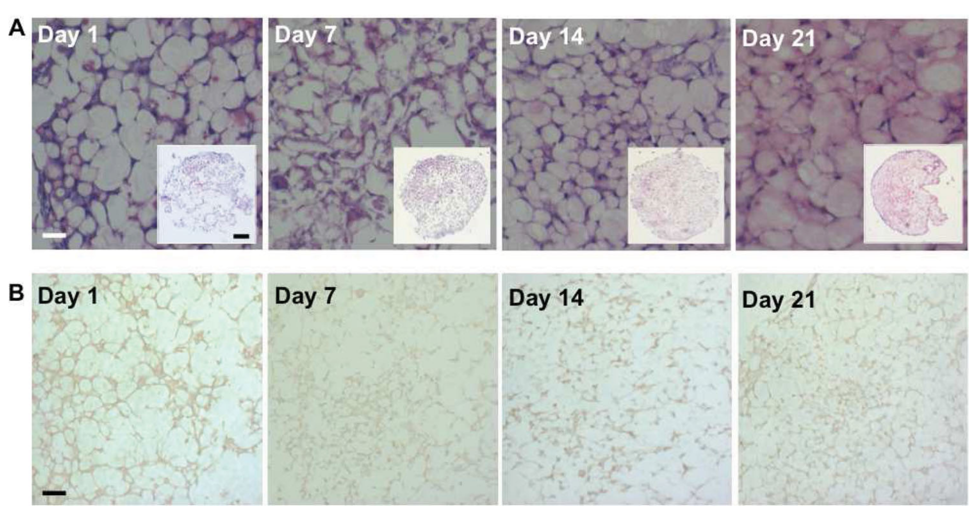

Figure 9. A) Light microscopy images of histological sections obtained from the constructs up to 21 days of culture stained for H&E. Insets show the overall structure of the constructs. B) Light microscopy images showing immunolocalisation of PDGF-BB obtained from the constructs up to 21 days of culture. Scale bars in the insets: 200 µm. Scale bars in high magnification pictures: 50 µm.

within the construct, indicating that the immobilization process was successful.

3. Discussion

Many strategies employed in regenerative therapies focus on mimicking the local microenvironment of tissues by using nanostructured matrices capable of providing 3D supports for stem cells.[37] The design criteria for the development of a bottom-up strategy must begin with building blocks assembled into higher order structures incorporating cells with appropriate signals for morphogenesis of the new tissue. Herein was investigated the cell behavior of hASCs seeded on functionalized chitosan μPs that work as building blocks and the ability of the system to assemble into a stable 3D construct allowing cell proliferation.

Surface primary amino-groups in the chitosan surface allow immobilization of ligands through amide-bond formation with carbodiimide-activated carboxylic groups.[38] EDC immobilization has been successfully used for the immobilization of antibodies and other proteins.[20,39,40] This study employed this method as a simple and reliable strategy to coat chitosan μPs with antibodies for targeting specific GFs in PLs.

In a previous report, PLs were used simultaneously as a source and carrier of GFs, assembling both functionalities into a 3D structural support.[41] This approach uses the assembly of nanoparticles, promoted by the adsorption of PLs to the surface of the nanoparticles, providing an adequate environment for the encapsulation of ASCs. Nevertheless, the complex composition of PLs can play simultaneously a positive and a negative role, as it makes it difficult to characterize the complex cocktail of molecules and to understand the mechanisms by which it influences cell behavior. Development of more controllable systems for the delivery of a characterized population of autologous GFs will certainly improve many clinical aspects on the use of PLs. The strategy herein described aims to recruit specific GFs, directing cell function and avoiding the implantation of an uncharacterized complex mixture that is not clear how it works.

Soluble GFs have been used in vitro to improve the properties of engineered tissues, however, immobilization is a promising approach for providing GF in a well-controlled manner, overcoming the diffusional limitations of soluble factors with an additional advantage of inducing local effects.[42,43] In this work, these signaling molecules are immobilized in the chitosan μPs, that work as building blocks providing localized and strong interactions between GFs and the resident cells.

The capture of GFs from PLs was assessed by ELISA assay on the remaining lysates solution post-incubation with the μPs (Figure 3). Unsurprisingly, PDGF-BB was the mostly recruited by the particles as anti-PDGF-BB was the antibody immobilized. Results clearly show a significant decrease in the amount of this GF in solution when compared to TFG-β1 and VEGF (Figure 3). The decrease in PDGF-BB represents a recruitment efficiency of around 68% against the 18% and 20% decrease in the values of TGF-β1 and VEGF respectively. TGF- β1 and VEGF recruited from the solution is certainly due to some adsorption on the particles or non-specific reactivity with anti-PDGF-BB. This provides evidence that the functionalization of the μPs is effective and they are rather selective for PDGF-BB. Therefore, this method allows the user to selectively functionalize the particles by binding specific single or combinations of antibodies onto the surface prior to incubation with PLs in order to select specific GFs.

Different GFs will certainly lead to different stem cell function and further differentiation towards a specific lineage. PDGFs are one of the GFs present in highest concentration in PLs..[23,24] Additionally PDGF is a principal chemo attractant for MSCs[32,33,44] and in particular PDGF-BB strongly induces the proliferation and migration of MSCs.[45,46] As a proof of concept was herein hypothesized that the functionalization with PDGF-BB will promote stem cell attachment and proliferation, leading to a formation of stable 3D structure. Having established that PDGF-BB was immobilized on the chitosan particles, the effect of this GF in the assembly process of a 3D structure was investigated. Ninety minutes after cell seeding it was possible to observe small “cloudy” aggregates, given rise to a more compact structure 24 hours after seeding (Figure 4a). After this time, most of the cells were viable and uniformly attached to the particles (Figure 4b). The controls used reveal low cell attachment and were not able to form a stable construct (Table 1). The fast attachment of cells to the μPs should be attributed to the PDGF-BB that is recognized by the cells due to specific cell surface receptors. These data suggest that hASCs can recognize and bind to the μPs leading to a stable assembly that allows cell spreading and growing. Cells act here as crosslinker agents inducing the formation of a stable construct. DMA analysis revealed that the storage modulus of the microgel increased by means of increasing frequency (Figure 5a). DMA data demonstrated an efficient reinforcement of the structure with increase in cell culture time, as shown by the remarkable increase in the storage modulus after 21 days of culture as compared to 14 days. Most probably, this outcome was caused by the large production of ECM that took place at this stage of culture, together with the compacting of the overall structure. The evolution of the storage modulus (E') with cell growth and extracellular matrix production has been reported in works regarding adipose stem cells encapsulation in hydrogels.[35,36] In both studies, a significant increase in the stiffness of the biomaterials-cells constructs was observed with increasing cell culture periods. The decrease of the loss factor (Figure 5b) indicates that the relative viscous component of the viscoelastic behavior is reduced, that could be also assigned to the loss of water and the densification of the construct. The values of E' upon 21 days of culture, above 150 kPa (for $f > 1$Hz) and the tan $\delta < 0.3$, indicate that the structures have good mechanical integrity and behave essentially as an elastic assembly.

The morphological observations by confocal microscopy and SEM in Figures 6, 7 clearly indicate that cells can spread around particles that organize and aggregate in a complex structure. The spherical 3D structure obtained evidences the capacity of the microgel to easily adapt to the shape of a defect or to be molded into a predesigned shape (Figure 7E). After 21 days is also possible to observe the increase in ECM deposition forming the typical fibrillar networks (Figure 7f). Moreover, the results suggest that the high cell density is apparent along the depth of the constructs (Figure 7f). The obtained structure with assembly of μPs and cells may enhance transport of nutrients, promoting efficient cell growth and tissue regeneration.

Live/dead assay to the construct after 21 days in culture indicate that cells are viable from the core to the outside of the construct. (Figure 8a,b) We believe that the enrichment of the particles with a specific GF strongly contributed for the overall positive cell viability within the core of the construct, typically one of the drawbacks found in these 3D cell encapsulation/entrapment systems.

Cell viability was significantly higher on day 3 when compared to longer incubation times (Figure 8c). The decline in fluorescence could be due to the inability of Alamar Blue to react with cells trapped within the compact construct as they migrate through the depth of the microgel where cells are not as readily available to react with this substance. The 3D structures are also increasingly dense with the accumulation of deposited ECM produced by the entrapped hASCs, thus limiting the diffusion ability of the reagent to assess the viability of the cells present in the inner parts of the microgel. Cell proliferation assay (Figure 8d) also showed significant enhancement on cell proliferation from day 14 to day 21, thus confirming the data obtained with the mechanical analysis. Results from cell proliferation imply that the 3D structures support cell grow and proliferation up to 21 days.

Histologically, it was observed that cells were grown in layers on the surface of the particles. These cultured particles clustered due to cell connecting points, giving rise to the constructs (Figure 9a). It was possible to observe that the cells were able to infiltrate, adhere, and proliferate into the inner parts of the constructs with an increased matrix deposition with increasing culture time. As evaluated via immunohistochemical analysis, immobilization of PDGF-BB within the construct was efficient as detected by the homogeneous distribution on the surface of the chitosan μPs within the construct. The observed increase of signal with culture time may be associated to the secretion of this GF by the entrapped cells (Figure 9b).

4. Conclusions

This study demonstrates the utility of GF-functionalized μPs as a strategy of forming instructive microenvironments for applications in TE. The proposed system offer different functionalities as the ability to target GFs from complex mixtures of bioactive proteins, which when combined with cells, are able to establish interconnected networks and lead to the formation of stable and robust 3D structures offering appropriate stimulus for cell culture. The herein presented microgels also present an injectability potential, appropriate for minimally invasive regenerative medicine approaches. These gels have the ability to gellify in situ just by the presence of cells, avoiding the performance of chemical reactions inside the body. The obtained construct simultaneously provides support for stem cell proliferation, as well as localized and sustained presentation of factors to modulate cell function. The presented methodology offers wide versatility as different formulations with a combination of GFs can be used for a particular application based on the desired composition and intended cellular function. Moreover therapeutic agents could be encapsulated in order to control cell differentiation. As a future perspective, further refinement of the microgel could be achieved by combining with specific GFs of interest with subsequent studies in stem cell differentiation.

5. Experimental Section

Microparticles Preparation: Medium molecular weight chitosan (Sigma, USA) was dissolved in a 2% v/v aqueous acetic acid solution with a final concentration of 1% w/v. Subsequently the chitosan solution was passed through an aerodynamically-assisted jetting equipment (Nisco Encapsulation Units VAR J30). The injected air led the chitosan solution to break up into a spray at the outlet of the nozzle. The generated microdroplets were hardened by a gelling process into a 1.0 M sodium hydroxide solution that resulted in the production of chitosan μPs. μPs were thoroughly washed and stored in PBS at 4 °C until further use.

Platelet Lysates Preparation: PLs were obtained from different apheresis collections performed at the Portuguese blood bank (IPS, Porto, Portugal). Samples were transferred to the laboratory within 24 h after collection and immediately submitted to three repeated temperature cycles (frozen with liquid nitrogen at –196 °C and heated at 37 °C), followed by a centrifugation step at 1400 *g* for 10 min, to eliminate the platelets debris. The lysates were then frozen at –20 °C until further use.

Microparticles Functionalization: μPs were modified with Alexa Fluor 488 Rabbit Anti-Mouse antibody (Invitrogen, USA) by 1-ethyl-3-(3-dimethylaminopropyl) carbodiimide hydrochloride (EDC) (Sigma, USA) chemistry. 500 μL of a 1 μg mL^{-1} antibody solution was pre-activated using EDC (2.0 mM) in PBS for 15 min, followed by incubation with 3 mg of chitosan μPs at 4 °C for 3 h. Particles were then washed at least 3× in PBS and observed under a fluorescence microscope (Zeiss HAL 100/HBO 100). For the modification with anti-human Platelet Derived Growth Factor-BB (PDGF-BB) (Peprotech) 500 μL of a 10 μg mL^{-1} antibody solution was pre-activated using EDC (2 mM) in PBS for 15 min, followed by incubation with 3 mg of chitosan μPs at 4 °C for 3 h. Particles were then washed at least 3× with PBS. The functionalization of the μPs with a specific GF, in this particular case PDGF-BB, was obtained by simply mixing the modified μPs with the PLs at 4 °C for 15 min. PLs solution was removed afterwards and the remaining GFs in the supernatant were quantified by ELISA assays.

Cell Seeding and Scaffold Assembly: Human adipose stem cells (hASCs) were isolated from human subcutaneous adipose tissue samples obtained from lipoaspiration procedures at Department of Plastic Surgery of Hospital da Prelada, Porto, Portugal. Human ASCs were enzymatically isolated from the adipose tissue samples as previously described.[47] The hASCs were cultured in alpha Medium (αMEM) supplemented with sodium bicarbonate, antibiotic/antimycotic and 10% FBS (complete medium). For cell seeding, 1×10^6 hASCs were mixed with 2×10^5 μPs in 500 μL complete medium and incubated at 37 °C, 5% CO_2. The assembly process was followed and imaged at different time points, up to 24 h. The samples were cultured for 21 days. Constructs were evaluated for cell proliferation, viability and processed for histological analysis, confocal microscopy and scanning electronic microscopy (SEM).

Dynamic Mechanical Analysis (DMA): The viscoelastic measurements of the constructs were performed using a TRITEC8000B DMA (Triton Technology, UK), equipped with the compressive mode. DMA spectra were obtained during a frequency scan ranging between 0.1 and 15 Hz for all time points. The experiments were performed under constant strain amplitude, corresponding to approximately 1% of the original height of the sample. Samples were tested under physiological-like conditions, i.e., immersed in PBS and at 37 °C.

Confocal Microscopy and Scanning Electronic Microscopic (SEM) Analysis: The constructs were fixed with 10% formalin in PBS. For confocal analysis, samples were stained with phalloidin (Sigma, USA) that binds to the cytoskeleton filaments, and DAPI (4,6-diamidino-

2-phenylindole, dilactate; Invitrogen, USA), which binds to DNA. Samples were washed and kept in PBS until confocal laser scanning microscopy analysis (Olympus Fluoview FV1000). For SEM analysis, fixed samples were dehydrated in a graded series of ethanol solutions, critical-point dried with carbon dioxide (Tousimis Autosamdri-815), sputtered with gold and evaluated by SEM (Leica Cambridge, Model S360, UK).

Cell Viability and Proliferation: Calcein AM/propidium iodide (PI) was performed after 1 day and after 21 days in culture. Briefly, the samples were incubated for 15 min with calcein AM (Invitrogen, USA) solution (2 μL calcein per mL αMEM without phenol red) and 100 μL of PI (Invitrogen, USA) solution (2 μL (stock solution of 1 mg mL^{-1}) in PBS). Samples were washed with PBS and observed under fluorescence microscopy (Zeiss HAL 100/HBO 100). Alamar Blue assay (Invitrogen, USA), was performed to determine cell viability at specific time points. Briefly, the constructs were incubated in cell culture medium supplemented with 10% Alamar Blue dye and allowed to incubate for 4 h. The fluorescence of the resulting solution was measured on a microplate reader (Sinergy HT, Bio-Tek Instruments, USA). Cell proliferation was determined by DNA quantification using a fluorimetric dsDNA quantification kit (PicoGreen, Invitrogen, USA). Samples collected after each time point were washed with PBS and immersed in 1 mL of ultrapure water, frozen for at –80 °C, thawed at room temperature, and sonicated for 30 min. Fluorescence was measured on a microplate reader (Sinergy HT, Bio-Tek Instruments, USA).

Histological Analysis: Constructs were collected at specific time points and fixed with 10% formalin in PBS. The constructs were included in paraffin and sections of 5 μm of thickness were obtained using a microtome (Micron HM355S, Thermo Scientific, Germany) and mounted in a micro-slide glass. Hematoxylin & Eosin (H&E) staining was performed using the automatic stainer (Micron HMS 740, Thermo Scientific, Germany). The slides were then mounted using Microscopy Entellan for observation under a light microscope (Zeiss HAL 100/HBO 100).

Immunohistochemistry: Immunostaining for PDGF-BB was performed to assess the presence of the immobilized GF on the surface of the particles. Antigen retrieval was heat induced in a water bath at 96 °C for 20 min, with incubation of the slides in citrate buffer (pH = 6). R.T.U. Vectastain Universal Elite ABC Kit (Vector, VCPK-7200) was used for antibody incubation, according to the instructions of the manufacturer. Briefly, sections were incubated with the primary antibody, anti-human PDGF-BB (Peprotech) overnight at 4 °C, in a humidified atmosphere. Control sections were incubated with 3% bovine serum albumin in PBS. After washing with PBS, antibody detection was revealed using the Peroxidase Substrate Kit DAB (Vector, VCSK-4100). All images were obtained using a light microscope (Zeiss HAL 100/HBO 100).

Statistical Analysis: All the experiments were performed with at least three replicates. Results are expressed as mean ± standard deviation. Differences between the experimental results were analyzed using the Student t-test, with the limit for statistical significance being defined as $p < 0.05$.

Acknowledgements

The research leading to these results has received funding from the European Union's Seventh Framework Programme (FP7/2007–2013) under grant agreement n° REGPOT-CT2012–316331-POLARIS. The authors acknowledge the Portuguese Foundation for Science and Technology (FCT) for the fellowships SFRH/BD/61390/2009 (C.A.C.) for the financial support. The authors are grateful to Hospital da Prelada for the lipoaspirates donations.

Received: May 3, 2013
Revised: September 20, 2013
Published online: November 4, 2013

[1] L. G. Griffith, M. A. Swartz, *Nat. Rev. Mol. Cell Biol.* **2006**, *7*, 211–224.
[2] R. Gauvin, A. Khademhosseini, *ACS Nano* **2011**, *5*, 4258–4264.
[3] T. G. Kim, H. Shin, D. W. Lim, *Adv. Funct. Mater.* **2012**, *22*, 2446–2468.
[4] Y. A. Du, E. Lo, S. Ali, A. Khademhosseini, *Proc. Natl. Acad. Sci. U. S. A.* **2008**, *105*, 9522–9527.
[5] J. G. Fernandez, A. Khademhosseini, *Adv. Mater.* **2010**, *22*, 2538–2541.
[6] F. Xu, C. A. M. Wu, V. Rengarajan, T. D. Finley, H. O. Keles, Y. R. Sung, B. Q. Li, U. A. Gurkan, U. Demirci, *Adv. Mater.* **2011**, *23*, 4254–4260.
[7] H. Shen, X. X. Hu, F. Yang, J. Z. Bei, S. G. Wang, *Acta Biomater.* **2010**, *6*, 455–465.
[8] H. P. Tan, J. D. Wu, D. J. Huang, C. Y. Gao, *Macromol. Biosci.* **2010**, *10*, 156–163.
[9] M. B. Oliveira, W. L. Song, L. Martin, S. M. Oliveira, S. G. Caridade, M. Alonso, J. C. Rodriguez-Cabello, J. F. Mano, *Soft Matter* **2011**, *7*, 6426–6434.
[10] W. H. Chen, Y. W. Tong, *Acta Biomater.* **2012**, *8*, 540–548.
[11] X. Q. Jia, Y. Yeo, R. J. Clifton, T. Jiao, D. S. Kohane, J. B. Kobler, S. M. Zeitels, R. Langer, *Biomacromolecules* **2006**, *7*, 3336–3344.
[12] N. R. Mercier, H. R. Costantino, M. A. Tracy, L. J. Bonassar, *Biomaterials* **2005**, *26*, 1945–1952.
[13] X. H. Liu, X. B. Jin, P. X. Ma, *Nat. Mater.* **2011**, *10*, 398–406.
[14] S. W. Kang, H. S. Yang, S. W. Seo, D. K. Han, B. S. Kim, *J. Biomed. Mater. Res. A* **2008**, *85A*, 747–756.
[15] H. J. Chung, T. G. Park, *Tissue Eng. Part A* **2009**, *15*, 1391–1400.
[16] A. Di Martino, M. Sittinger, M. V. Risbud, *Biomaterials* **2005**, *26*, 5983–5990.
[17] N. M. Alves, J. F. Mano, *Int. J. Biol. Macromol.* **2008**, *43*, 401–414.
[18] T. W. Chung, Y. F. Lu, S. S. Wang, Y. S. Lin, S. H. Chu, *Biomaterials* **2002**, *23*, 4803–4809.
[19] J. T. Zhang, J. Q. Nie, M. Muhlstadt, H. Gallagher, O. Pullig, K. D. Jandt, *Adv. Funct. Mater.* **2011**, *21*, 4079–4087.
[20] C. A. Custodio, C. M. Alves, R. L. Reis, J. F. Mano, *J. Tissue Eng. Regener. Med.* **2010**, *4*, 316–323.
[21] D. J. Soomekh, *Clin. Podiatr. Med. Surg.* **2011**, *28*, 155–170.
[22] V. E. Santo, M. E. Gomes, J. F. Mano, R. L. Reis, *J. Tissue Eng. Regener. Med.* **2012**, *6*, s47–s59.
[23] M. E. Doumit, D. R. Cook, R. A. Merkel, *J. Cell Physiol.* **1993**, *157*, 326–332.
[24] F. Ng, S. Boucher, S. Koh, K. S. R. Sastry, L. Chase, U. Lakshmipathy, C. Choong, Z. Yang, M. C. Vemuri, M. S. Rao, V. Tanavde, *Blood* **2008**, *112*, 295–307.
[25] C. Doucet, I. Ernou, Y. Z. Zhang, J. R. Llense, L. Begot, X. Holy, J. J. Lataillade, *J Cell Physiol.* **2005**, *205*, 228–236.
[26] C. Bertoldi, M. Pinti, D. Zaffe, A. Cossarizza, U. Consolo, G. B. Ceccherelli, *Transfusion* **2009**, *49*, 1728–1737.
[27] M. Lohmann, G. Walenda, H. Hemeda, S. Joussen, W. Drescher, S. Jockenhoevel, G. Hutschenreuter, M. Zenke, W. Wagner, *PLoS One* **2012**, *7*, e37839.
[28] F. M. Chen, M. Zhang, Z. F. Wu, *Biomaterials* **2010**, *31*, 6279–6308.
[29] P. A. Zuk, M. Zhu, P. Ashjian, D. A. De Ugarte, J. I. Huang, H. Mizuno, Z. C. Alfonso, J. K. Fraser, P. Benhaim, M. H. Hedrick, *Mol. Biol. Cell* **2002**, *13*, 4279–4295.
[30] J. M. Gimble, A. J. Katz, B. A. Bunnell, *Circ. Res.* **2007**, *100*, 1249–1260.
[31] B. Lindroos, R. Suuronen, S. Miettinen, *Stem Cell Rev. Rep.* **2011**, *7*, 269–291.
[32] C. H. Heldin, B. Westermark, *Physiol. Rev.* **1999**, *79*, 1283–1316.
[33] J. Fiedler, G. Roderer, K. P. Gunther, R. E. Brenner, *J. Cell Biochem.* **2002**, *87*, 305–312.

[34] D. M. G. Cruz, J. L. E. Ivirico, M. M. Gomes, J. L. G. Ribelles, M. S. Sanchez, R. L. Reis, J. F. Mano, *J. Tissue Eng. Regener. Med.* **2008**, *2*, 378–380.
[35] E. G. Popa, M. T. Rodrigues, D. F. Coutinho, M. B. Oliveira, J. F. Mano, R. L. Reis, M. E. Gomes, *Soft Matter* **2013**, *9*, 875–885.
[36] J. Silva-Correia, A. Gloria, M. B. Oliveira, J. F. Mano, J. M. Oliveira, L. Ambrosio, R. L. Reis, *J. Biomed. Mater. Res. A* **2013**, DOI: 10.1002/jbm.a.34650.
[37] F. Gelain, *Int. J. Nanomed.* **2008**, *3*, 415–424.
[38] G. T. Hermanson, *Bioconjugate techniques* 2nd ed., Elsevier, USA, **1996**.
[39] L. L. Y. Chiu, R. D. Weisel, R. K. Li, M. Radisic, *J. Tissue Eng. Regener. Med.* **2011**, *5*, 69–84.
[40] B. Masereel, M. Dinguizli, C. Bouzin, N. Moniotte, O. Feron, B. Gallez, T. V. Borght, C. Michiels, S. Lucas, *J. Nanopart. Res.* **2011**, *13*, 1573–1580.
[41] V. E. Santo, E. G. Popa, M. E. Gomes, J. F. Mano, R. L. Reis, *Histol. Histopathol. Cell. Mol. Biol.* **2011**, *26*, 164.
[42] Y. Ito, *Mat. Sci. Eng. C* **1998**, *6*, 267–274.
[43] V. E. Santo, M. E. Gomes, J. F. Mano, R. L. Reis, *Nanomedicine* **2012**, *7*, 1045–1066.
[44] Y. J. Kang, E. S. Jeon, H. Y. Song, J. S. Woo, J. S. Jung, Y. K. Kim, J. H. Kim, *J. Cell Biochem.* **2005**, *95*, 1135–1145.
[45] R. V. Hoch, P. Soriano, *Development* **2003**, *130*, 4769–4784.
[46] J. Andrae, R. Gallini, C. Betsholtz, *Gene Dev.* **2008**, *22*, 1276–1312.
[47] T. Rada, R. L. Reis, M. E. Gomes, *Stem Cell Rev. Rep.* **2011**, *7*, 64–76.